Developmental changes in calcium/calmodulin-dependent inactivation of calcium currents at the rat calyx of Held

Takeshi Nakamura[1], Takayuki Yamashita[1,3], Naoto Saitoh[1,2] and Tomoyuki Takahashi[1,2,3]

[1]*Department of Neurophysiology, University of Tokyo Graduate School of Medicine, Tokyo 113-0033, Japan*
[2]*Department of Neurophysiology, Doshisha University Faculty of Life and Medical Sciences, Kyoto 619-0225, Japan*
[3]*Cellular & Molecular Synaptic Function Unit, Initial Research Project (IRP), Okinawa Institute of Science and Technology Promotion Corporation (OIST), Okinawa 904-2234, Japan*

Ca^{2+}-binding to calmodulin (CaM) causes facilitation and/or inactivation of recombinant Ca^{2+} channels. At the rat calyx of Held, before hearing onset, presynaptic Ca^{2+} currents (I_{pCa}) undergo Ca^{2+}/CaM-dependent inactivation during repetitive activation at around 1 Hz, implying that this may be a major cause of short-term synaptic depression. However, it remains open whether the Ca^{2+}/CaM-dependent inactivation of I_{pCa} persists in more mature animals. To address this question, we tested the effect of CaM inhibitors on the activity-dependent modulation of I_{pCa} in calyces, before (postnatal day (P) 7–9) and after (P13–15) hearing onset. Our results indicate that the CaM-dependent I_{pCa} inactivation during low-frequency stimulation, and the ensuing synaptic depression, occur only at calyces in the prehearing period. However, CaM immunoreactivity in P8 and P14 calyces was equally strong. Even at P13–15, high frequency stimulation (200–500 Hz) could induce I_{pCa} inactivation, which was attenuated by EGTA (10 mM) or a CaM inhibitor peptide loaded into the terminal. Furthermore, the CaM inhibitor peptide attenuated a transient facilitation of I_{pCa} preceding inactivation observed at 500 Hz stimulation, whereas it had no effect on sustained I_{pCa} facilitations during trains of 50–200 Hz stimulation. These results suggest that the Ca^{2+}/CaM-dependent I_{pCa} modulation requires a high intraterminal Ca^{2+} concentration, which can be attained at immature calyces during low frequency stimulation, but only during unusually high frequency stimulation at calyceal terminals in the posthearing period.

(Received 6 August 2007; accepted after revision 25 January 2008; first published online 31 January 2008)
Corresponding author T. Takahashi: Doshisha University, Faculty of Life and Medical Sciences, Kyoto 619-0225, Japan. Email: ttakahas@mail.doshisha.ac.jp

At the calyx of Held synapse in the rodent auditory brainstem, repetitive activation at high frequencies (> 50 Hz) causes presynaptic Ca^{2+} currents (I_{pCa}) to undergo Ca^{2+}-dependent facilitation (Borst & Sakmann, 1998; Cuttle *et al.* 1998; Taschenberger *et al.* 2002; Tsujimoto *et al.* 2002) followed by divalent charge-carrier-dependent inactivation (Forsythe *et al.* 1998). This activity-dependent modulation of I_{pCa} contributes to short-term synaptic plasticity (Forsythe *et al.* 1998; Inchauspe *et al.* 2004; Ishikawa *et al.* 2005; for a review, see Takahashi, 2005). When activated at low frequencies (< 10 Hz), I_{pCa} remains unchanged in P14–17 rats (Takahashi *et al.* 2000). Recently, however, Xu & Wu (2005) reported that I_{pCa} undergoes strong inactivation during low frequency activation, such as 2 Hz, at P8–13 rat calyces. This I_{pCa} inactivation is Ca^{2+}/CaM dependent, and could be a major cause of short-term synaptic depression.

During the second postnatal week, during which hearing onset occurs (P10–12, Jewett & Romano, 1972; Futai *et al.* 2001), calyces of Held undergo dramatic morphological, molecular and functional changes (Kandler & Friauf, 1993; Taschenberger & von Gersdorff, 2000; Futai *et al.* 2001; Iwasaki & Takahashi, 2001; Taschenberger *et al.* 2002; Fedchyshyn & Wang, 2005). During this period, Ca^{2+} channel subtypes in the nerve terminal, which mediate transmitter release, switch from mixed N-, P/Q- and R-types to predominantly P/Q-type (Iwasaki & Takahashi, 1998; Iwasaki *et al.* 2000), mobile Ca^{2+} buffer proteins, such as parvalbumin and calretinin, increase (Felmy & Schneggenburger, 2004), and Ca^{2+}-dependent transmitter release modality changes (Fedchyshyn & Wang, 2005). As these developmental changes may potentially affect Ca^{2+}/CaM-dependent

T. Nakamura and T. Yamashita contributed equally to this work.

DOI: 10.1113/jphysiol.2007.142521

I_{pCa} inactivation, we examined I_{pCa} inactivation more closely, and compared calyces in prehearing (P7–9) and posthearing (P13–15) periods. Our results indicate that at the calyx of Held, the occurrence of Ca^{2+}/CaM-dependent inactivation of I_{pCa} during low frequency activation and its contribution to synaptic depression are developmental phenomena restricted to the prehearing period, and that after the second postnatal week, the CaM-dependent I_{pCa} inactivation can be induced only by the maximal frequency of stimulation.

Methods

Slice preparation and solutions

All experiments were performed in accordance with the guidelines of the Physiological Society of Japan. Brainstem slices were prepared from Wistar rats (P7–9 or P13–15) as previously described (Yamashita *et al.* 2003). Briefly, the rat was decapitated under halothane anaesthesia and the brain was quickly removed. Transverse slices (150–300 μm thick) containing the medial nucleus of the trapezoid body (MNTB) were cut using a tissue slicer (Linearslicer PRO-7; Dosaka, Japan).

Slices were incubated for 1 h at 36–37°C in artificial cerebrospinal fluid (aCSF) containing (mM): 125 NaCl, 2.5 KCl, 26 $NaHCO_3$, 1.25 NaH_2PO_4, 2 $CaCl_2$, 1 $MgCl_2$, 10 glucose, 3 *myo*-inositol, 2 sodium pyruvate, and 0.5 ascorbic acid (pH 7.4 when bubbled with 95% O_2 and 5% CO_2, 310–320 mosmol l^{-1}), and maintained thereafter at room temperature (22–28°C). All recordings were made at room temperature. The aCSF routinely contained bicuculline methiodide (10 μM) and strychnine hydrochloride (0.5 μM) to block $GABA_A$ receptors and glycine receptors, respectively. For measuring I_{pCa}, NaCl in the aCSF was replaced by equimolar TEA-Cl (10 mM). Furthermore, TTX (1 μM) and 4-AP (0.5 mM) were added to the aCSF to block sodium and potassium currents. The presynaptic pipette solutions contained (mM): 105 caesium gluconate, 30 CsCl, 10 Hepes, 0.5 EGTA, 1 $MgCl_2$, 12 phosphocreatine (Na salt), 3 ATP (Mg salt), 0.3 GTP (Na salt) (pH 7.3–7.4 adjusted with CsOH, 290–300 mosmol l^{-1}). In some experiments, myosin light chain kinase (MLCK) peptide (30 μM; Calbiochem, USA) was dissolved in the presynaptic pipette solution and loaded into the presynaptic terminal by diffusion. When 10 mM EGTA was added to the pipette solution, caesium gluconate was reduced to maintain constant osmolarity. The postsynaptic pipette solution contained (mM): 110 CsF, 30 CsCl, 10 Hepes, 5 EGTA, 1 $MgCl_2$ and 5 QX-314 (pH adjusted to 7.3–7.4 with CsOH, 285–295 mosmol l^{-1}). For measuring EPSCs, D(−)2-amino-5-phosphonovaleric acid (D-APV, 50 μM) was added to the aCSF to block NMDA receptor-mediated currents. At P7–9 (but not at P13–15) calyceal synapses, AMPA receptor desensitization and saturation are involved in synaptic depression during repetitive stimulation (Taschenberger *et al.* 2002). To minimize these effects, cyclothiazide (100 μM) and kynurenate (2 mM) were included in the aCSF for recording EPSCs in P7–9 rats.

Recordings and data analysis

Whole-cell recordings were made from the calyx of Held presynaptic terminals and postsynaptic MNTB principal neurons using a patch-clamp amplifier (EPC 7 or EPC 9/2, HEKA Electronik, Germany) as previously described (Yamashita *et al.* 2003). The presynaptic pipette was pulled to give a resistance of 5–7 MΩ and recordings had a series resistance of 9–25 MΩ, which was compensated by up to 75% for a final value of 6–7 MΩ. Presynaptic Ca^{2+} currents were evoked by 1 ms depolarizing command pulses to 0 mV under voltage-clamp at a holding potential of −80 mV unless otherwise noted. The resistance of the postsynaptic pipette was 2–4 MΩ, and series resistance was typically 7–15 MΩ, which was not compensated for.

EPSCs were evoked by afferent fibre stimulation with a bipolar tungsten electrode positioned halfway between the midline and the MNTB. Records were low-pass filtered at 5 kHz and digitized at 50 kHz. To examine the effect of calmidazolium on I_{pCa} and EPSCs, we incubated slices with aCSF containing calmidazolium (20 μM; Sigma, USA) at least 30 min before and during recordings. Calmidazolium had no effect on the basal amplitude of I_{pCa} and EPSCs (data not shown).

All values are given as means ± S.E.M. and significance of difference was evaluated by Student's unpaired *t* test or two-way ANOVA. $P < 0.05$ was taken as the level of significance.

Immunocytochemistry

Tissue fixation and immunocytochemistry of brainstem containing the MNTB region of Wistar rats (P8 and P14) were performed as previously described (Ishikawa *et al.* 2003). To visualize CaM and synaptophysin, we used anti-CaM antibody (mouse monoclonal, Upstate Biotechnology, USA; diluted 1 : 500) and anti-synaptophysin antibody (rabbit polyclonal, Zymed Laboratories, USA; diluted 1 : 200), together with goat secondary antibodies conjugated with Alexa fluor 488 and Alexa fluor 588 (Invitrogen, USA; diluted 1 : 200). In the primary antibody absorbing tests for evaluating the specificity of the CaM immuno-reactivity, both recombinant CaM (Upstate) and CaM from bovine brain (Calbiochem) were incubated with primary antibodies for 30 min at room temperature.

Results

Developmental changes in CaM-dependent inactivation of presynaptic Ca^{2+} currents

I_{pCa} at P8–13 calyces undergoes inactivation during low frequency stimulation when recorded with a whole-cell pipette solution containing 50 μM BAPTA (Xu & Wu, 2005), whereas no such inactivation is observed for I_{pCa} at P14–17 calyces with a pipette solution containing 0.5 mM EGTA (Takahashi *et al.* 2000). To investigate whether the discrepancy between these results reflected the different Ca^{2+} buffer strengths in the pipette solutions, we evoked I_{pCa} at P7–9 calyces, under whole-cell voltage-clamp, with a pipette solution containing 0.5 mM EGTA, using a pair of brief (1 ms) depolarizing pulses (from −80 mV to 0 mV). In this protocol, I_{pCa} showed paired-pulse inactivation (PPI) at interstimulus interval (ISIs) of 0.05–2 s (Fig. 1*A* and *B*). The maximal inhibition (15.6 ± 2.4%, $n = 6$) was observed at 0.5 s ISI. Preincubation of slices with the CaM inhibitor calmidazolium (20 μM) significantly attenuated the PPI of I_{pCa}. Furthermore, intraterminal application of the myosin light chain kinase (MLCK) peptide (30 μM), a specific inhibitor of CaM (Török & Trentham, 1994), also attenuated the PPI of I_{pCa}. These results are consistent with those reported by Xu & Wu (2005), indicating that the Ca^{2+}/CaM-dependent inactivation of I_{pCa} is reproducible at P7–9 calyces with a pipette solution containing 0.5 mM EGTA.

We next investigated whether the CaM-dependent I_{pCa} inactivation persists after hearing onset (Jewett & Romano, 1972). At P13–15 calyces, I_{pCa} exhibited much less PPI (at 0.01–20 s ISIs, Fig. 1*C* and *D*). Neither calmidazolium (20 μM) nor MLCK peptide (30 μM) affected the PPI of I_{pCa}. These results indicate that the Ca^{2+}/CaM-dependent I_{pCa} inactivation at 0.1–2 s ISI is a developmental phenomenon, occurring only at immature calyces of Held.

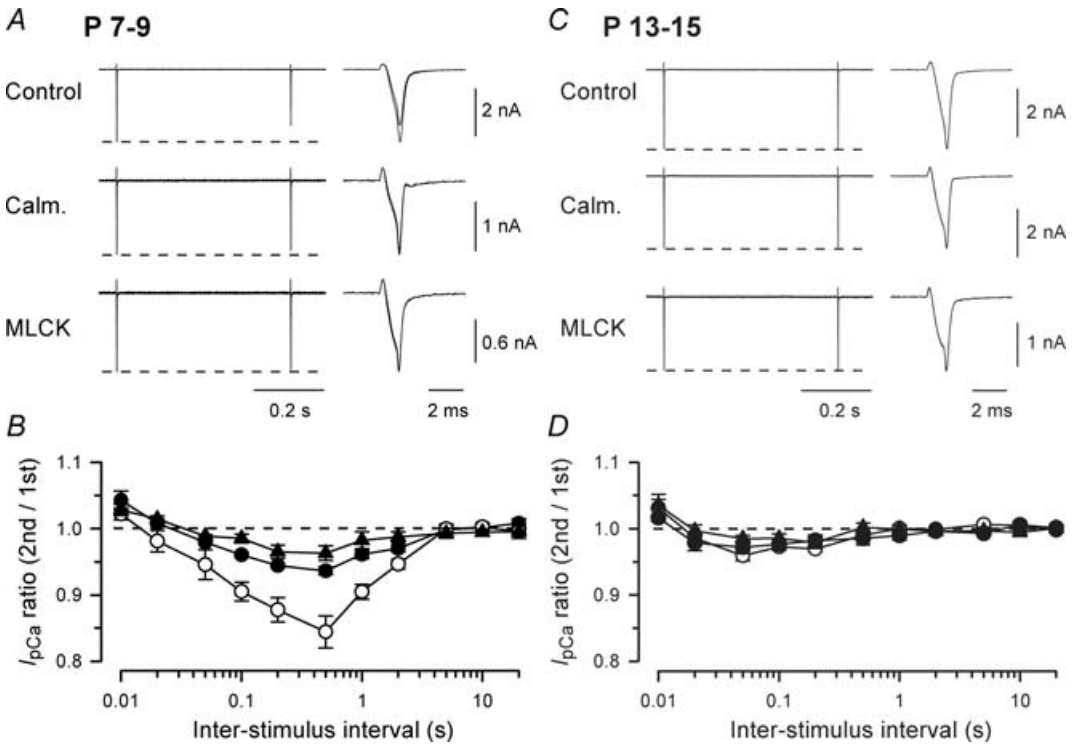

Figure 1. Developmental changes in I_{pCa} inactivation at the calyx of Held
I_{pCa} was induced by paired depolarizing command pulses (from −80 mV to 0 mV, 1 ms in duration) in P7–9 (*A* and *B*) or P13–15 (*C* and *D*) rat calyces. *A* and *C*, sample records of I_{pCa} after application of calmidazolium (Calm. 20 μM by preincubation), or MLCK peptide (MLCK, 30 μM, by intraterminal application), or without application of CaM inhibitors (Control). The fist and second I_{pCa} are superimposed on the right panel at faster time scales. Dashed lines indicate the first I_{pCa} amplitudes. *B* and *D*, the ratio of the second I_{pCa} amplitude relative to the first one (I_{pCa} ratio on ordinate) at different ISIs (abscissa) after calmidazolium treatment (●), intraterminal application of MLCK peptide (▲) or with no inhibitor application (○). At P7–9 (*B*), maximal I_{pCa} inactivation (at 0.5 s ISI) was 15.6 ± 2.4% ($n = 6$) in control, 6.4 ± 0.6% ($n = 5$) after calmidazolium treatment, and 3.7 ± 1.1% ($n = 5$) after intraterminal MLCK peptide application. At P13–15 (*D*), maximal I_{pCa} inactivation (at 50 ms ISI) was 4.1 ± 0.7% ($n = 7$) in control, 2.8 ± 1.0% ($n = 4$) after calmidazolium treatment, and 1.5 ± 0.5% ($n = 5$) after intraterminal MLCK peptide application. Results were essentially the same when the charge instead of amplitude was measured for I_{pCa}. In this and following figures, data points and bars indicate mean and S.E.M.

Contribution of CaM-dependent I_{pCa} inactivation to synaptic depression

In simultaneous pre- and postsynaptic whole-cell recording at P7–9 calyces, the Ca^{2+}/CaM-dependent I_{pCa} inactivation has been shown to contribute to synaptic depression during low frequency stimulation (Xu & Wu, 2005). However, under whole-cell recording, mobile endogenous Ca^{2+} buffers in the nerve terminal may be washed out and replaced by Ca^{2+} buffer in the pipette solution. To evaluate the contribution of Ca^{2+}/CaM-dependent I_{pCa} to synaptic depression at synapses with no presynaptic dialysis, we used calmidazolium, which inhibits Ca^{2+}/CaM-dependent I_{pCa} inactivation following extracellular application (Fig. 1). When EPSCs were evoked by afferent fibre stimulation at 0.5–5 Hz, they were depressed to a low steady level (Fig. 2*A*), which was lower at higher frequency of stimulation (Fig. 2*B*). Calmidazolium significantly attenuated the magnitude of synaptic depression, raising

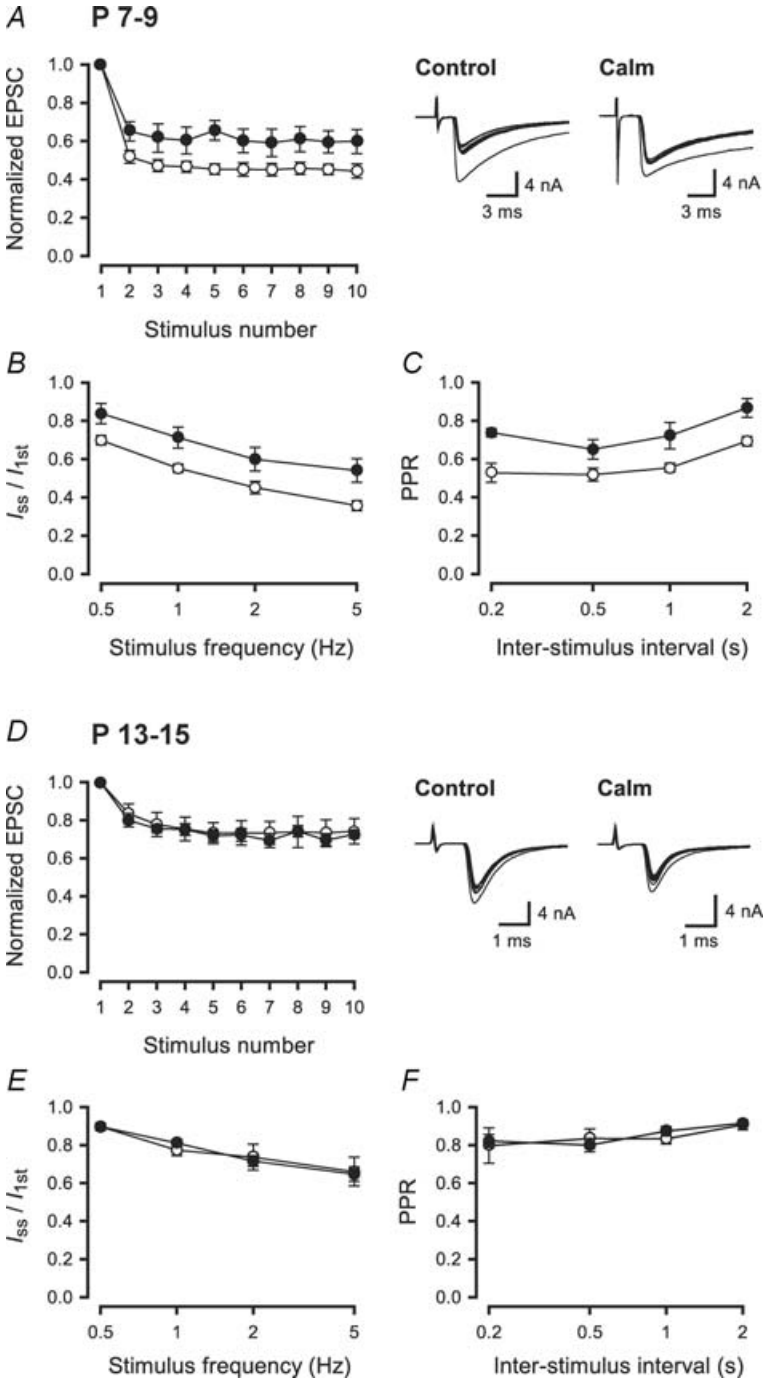

Figure 2. Developmental changes in the contribution of Ca^{2+}/CaM-dependent I_{pCa} inactivation to synaptic depression at the calyx of Held

Nerve-evoked EPSCs were recorded from MNTB principal neurons in P7–9 (*A*–*C*) and P13–15 (*D*–*F*) rats. *A* and *D*, the EPSC amplitudes, during a 2 Hz train (10 stimuli), relative to the first one, with (●) or without (○) calmidazolium pretreatment. Sample records show the 1st–10th EPSCs (superimposed). In *A*, cyclothiazide (100 μM) and kynurenate (2 mM) were included in the aCSF to block AMPA receptor desensitization and saturation. *B* and *E*, magnitude of synaptic depression, at P7–9 (*B*) and P13–15 (*E*) synapses, during trains of stimulation at 0.5–5 Hz, expressed as the steady-state amplitude (I_{ss}; mean of the 6th to 10th events) relative to the first EPSC amplitude (I_{1st}) with (●) or without (○) calmidazolium pretreatment. Calmidazolium significantly reduced the magnitude of synaptic depression ($P < 0.01$, $n = 5$–9) at P7–9 synapses (*B*), but had no effect at P13–14 synapses (*E*, $P > 0.9$, $n = 4$–9). *C* and *F*, paired-pulse ratio (PPR) of EPSCs at different ISIs with (●) or without (○) calmidazolium pretreatment at P7–9 (*C*) and P13–15 (*F*) synapses. The PPR was measured as the ratio of the second EPSC amplitude relative to the first one during trains of stimulation at different frequencies.

the steady level during repetitive stimulation, by 13–19% (Fig. 2*B*) and paired-pulse ratio of EPSCs by 13–21% (Fig. 2*C*). These results suggest that Ca^{2+}/CaM-dependent I_{pCa} inactivation does contribute to synaptic depression at P7–9 calyceal synapse, as postulated by Xu & Wu (2005). At P13–15, however, calmidazolium (20 μM) no longer attenuated synaptic depression (Fig. 2*D–F*), as expected from the lack of CaM-dependent I_{pCa} inactivation (Fig. 1*C* and *D*). Thus, the occurrence of Ca^{2+}/CaM-dependent I_{pCa} inactivation during low frequency stimulation and the ensuing synaptic depression are restricted to the prehearing period.

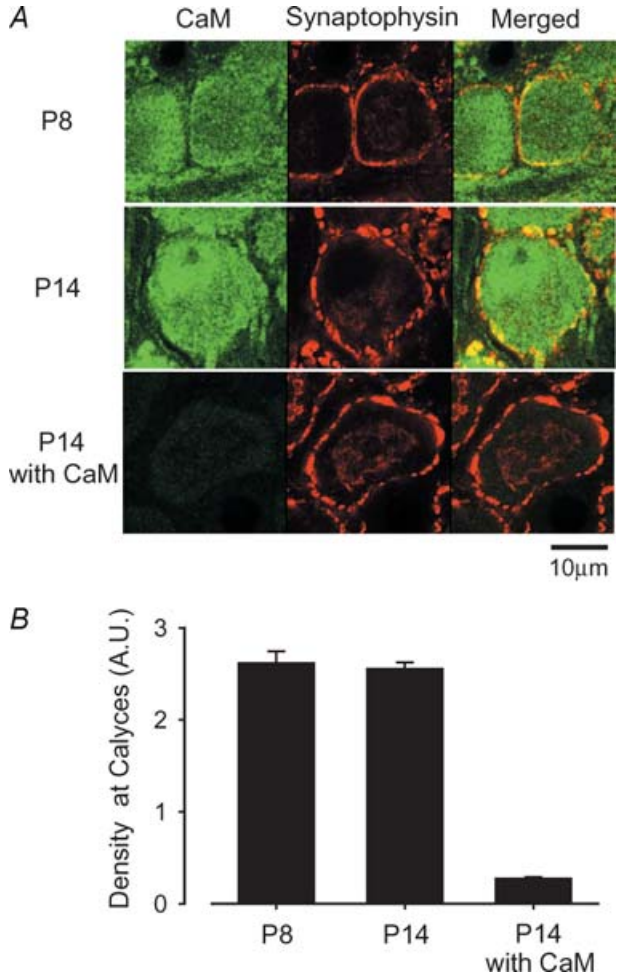

Figure 3. CaM immunoreactivities at the calyces of Held terminal at P8 and P14
A, CaM immunoreactivity (left column, labelled green with Alexa fluor 488), synaptophysin immunoreactivity (middle column, labelled red with Alexa fluor 568), and their overlap (right column, yellow). Bottom panel in the left column (P14 with CaM) shows the background after absorbing the primary antibodies with CaM protein. *B*, densitometric measurements of CaM immunofluorescence intensity in the regions overlapped with synaptophysin immunofluorescence signals at P8 and P14, and the background intensity after antibody absorption at P14.

Mechanisms underlying the developmental decline of CaM-dependent I_{pCa} inactivation

What mechanisms underlie the developmental decline of Ca^{2+}/CaM-dependent I_{pCa} inactivation? Might CaM expression in the nerve terminal be down-regulated during development? Presynaptic terminals, identified with synaptophysin immunoreactivity, as well as postsynaptic cell bodies, showed strong CaM-immunoreactivity at both P8 and P14 (Fig. 3*A*). The CaM-immunofluorescence signals were observed practically in all calyces in the MNTB region. The CaM-specificity of the signals was verified by their disappearance after absorbing the primary antibody with CaM protein (P14 with CaM). The average intensity of CaM-immunofluorescence signals at P14 calyces was similar to that at P8 calyces (Fig. 3*B*), indicating that the level of CaM expression in the nerve terminal was unchanged during the second postnatal week.

Ca^{2+} channel subtypes in calyceal terminals undergo a developmental switch from mixed N-, P/Q- and R-types to predominantly P/Q-type during the second postnatal week (Iwasaki & Takahashi, 1998; Iwasaki *et al.* 2000). We investigated whether this switch might be a cause for the reduction of CaM-dependent I_{pCa} inactivation. At P7–9 calyces, after blocking N-type VGCCs using ω-conotoxin GVIA (2 μM), I_{pCa} clearly showed PPI with its peak being observed at 0.5 s ISI (Fig. 4). The magnitude of inactivation was, however, slightly smaller than control, presumably because of less Ca^{2+} influx after blocking N-type VGCCs. These results indicate that the developmental reduction of N-type VGCCs cannot be a major cause for the developmental decline of CaM-dependent I_{pCa} inactivation.

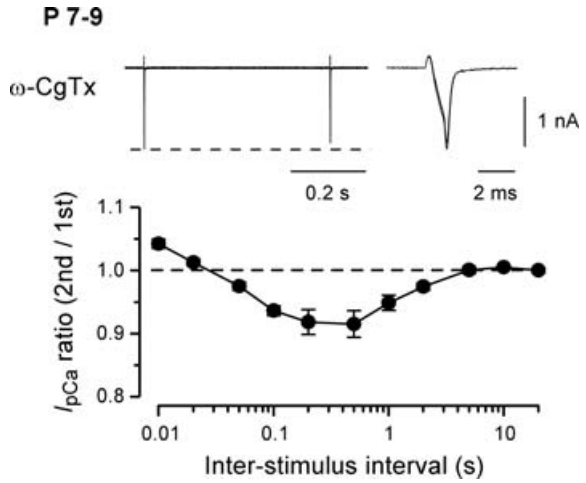

Figure 4. Effect of an N-type Ca^{2+} channel blocker on the Ca^{2+}/CaM-dependent inactivation of I_{pCa}
I_{pCa} was induced by paired depolarizing pulses, as in Fig. 1, in the presence of ω-CgTX (2 μM) at P7–9 calyces ($n = 5$). Sample records, and the ratio of the second I_{pCa} amplitude relative to the first one at different ISIs (abscissa), are shown as in Fig. 1.

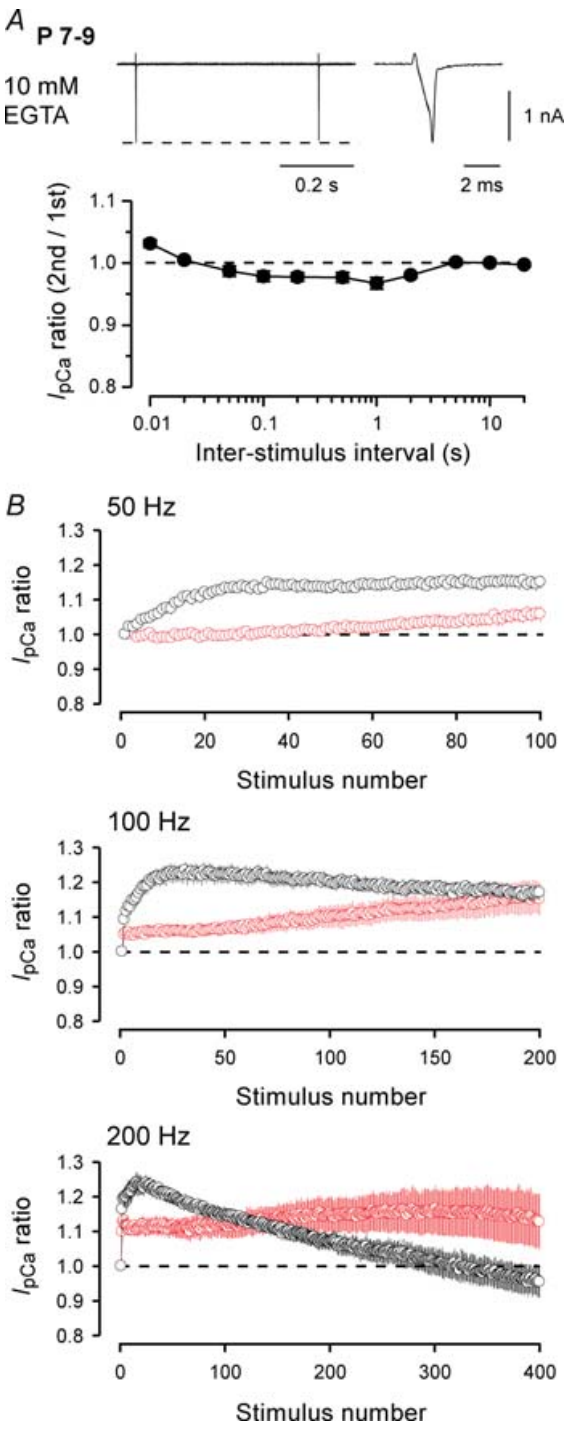

Figure 5. Inhibitory effects of EGTA on the activity-dependent inactivation and facilitation of I_{pCa}
I_{pCa} was evoked by 1 ms depolarizing command pulses after dialysing calyces with a patch pipette solution containing 10 mM EGTA. *A*, at P7–9 calyces, EGTA markedly reduced I_{pCa} inactivation induced by the paired-pulse protocol. The maximal I_{pCa} inactivation (at 1 s ISI) was $3.3 \pm 0.8\%$ ($n = 5$), which was significantly less than control in Fig. 1 ($P < 0.01$). *B,* at P13–15 calyces, I_{pCa} was evoked by 2 s trains of 1 ms command pulses at 50 Hz, 100 Hz and 200 Hz, with 0.5 mM (black, $n = 4$) or 10 mM (red, $n = 4$) EGTA included in the patch pipette solution. On the ordinate, the I_{pCa} amplitude is normalized to the initial one.

Binding of Ca^{2+} to the C-terminal lobe of CaM facilitates VGCCs (Ca^{2+}-dependent facilitation, CDF), whereas Ca^{2+} binding to its N-terminal lobe inactivates VGCCs (Ca^{2+}-dependent inactivation, CDI) (DeMaria *et al.* 2001; Liang *et al.* 2003). In cells expressed with recombinant P/Q-type channels, intracellular EGTA has no effect on C-lobe-dependent CDF but blocks N-lobe-dependent CDI (Liang *et al.* 2003; see also Lee *et al.* 2000). Whilst it remains open whether such a differential mechanism operates for native VGCCs, we examined whether EGTA affects Ca^{2+}/CaM-dependent inactivation of I_{pCa} at P7–9 calyces. As shown in Fig. 5*A*, EGTA (10 mM) markedly reduced Ca^{2+}/CaM-dependent inactivation of I_{pCa}, suggesting that CaM N-lobe might be involved in I_{pCa} inactivation. Because EGTA has a slow binding on-rate (Smith *et al.* 1984) it can reduce Ca^{2+} mainly in the region distant from the site of Ca^{2+} entry. Might it be that even in mature calyces, if Ca^{2+} accumulates during high frequency stimulation, I_{pCa} undergoes Ca^{2+}/CaM-dependent inactivation? When we repetitively activated I_{pCa} by 1 ms depolarizing square pulses at 50–200 Hz for 2 s, I_{pCa} underwent facilitation, which was followed by inactivation at 200 Hz. EGTA (10 mM) loaded into calyces attenuated both facilitation and inactivation of I_{pCa} (Fig. 5*B*). Thus, the Ca^{2+}-dependent inactivation of I_{pCa} can be induced in mature calyces even after hearing onset.

We next investigated whether the I_{pCa} modulation observed during trains of repetitive stimulation at mature calyces was CaM dependent. In these experiments we evoked I_{pCa} by trains of action potential (AP)-waveform pulses (Fig. 6*A*). With this protocol I_{pCa} showed predominant facilitation during stimulation at 50–200 Hz (Fig. 6*B–D*), but a sustained inactivation followed a transient facilitation when stimulated at 500 Hz (Fig. 6*E*). MLCK peptide (30 μM), loaded into calyces, had no effect on I_{pCa} facilitation at 50–200 Hz, but attenuated both facilitation and inactivation of I_{pCa} at 500 Hz.

Discussion

Developmental decline of Ca^{2+}/CaM-dependent I_{pCa} inactivation

At immature calyces of Held (P7–9), we confirmed the findings by Xu & Wu (2005) that I_{pCa} evoked by a pair of brief depolarizing pulses undergoes prominent PPI at long ISIs (0.05–2 s), and that these PPI can be attenuated by the CaM inhibitors calmidazolium or MLCK peptide. In contrast, at P13–15 calyces, the Ca^{2+}/CaM-dependent PPI of I_{pCa} was absent, despite the fact that CaM expression in calyceal terminals was similar at P8 and P14. Even at P13–15, however, repetitive activation of I_{pCa} at high frequencies showed I_{pCa} inactivation, which could be attenuated by 10 mM EGTA or MLCK peptide. These

results suggest that the developmental decline of the Ca^{2+}/CaM-dependent inactivation of I_{pCa} results from a developmental change in the intraterminal Ca^{2+} dynamics, rather than the Ca^{2+}/CaM-dependent mechanism.

CaM has four Ca^{2+} binding sites with K_d ranging from 1.7 μM to 8.9 μM (Shifman *et al.* 2006). At P8–10 calyces, the volume-averaged intraterminal Ca^{2+} concentration reaches 400 nM during an AP (Helmchen *et al.* 1997). After hearing onset, local Ca^{2+} transients, evoked by an AP and assessed by confocal spot measurements, become sparser and smaller (Nakamura *et al.* 2007). Developmental changes in intraterminal Ca^{2+} dynamics have been suggested by the finding that 10 mM EGTA loaded into calyces reduces EPSCs by more than 50% in the prehearing period (Borst & Sakmann, 1996), but that the reduction becomes marginal after hearing onset, despite the fact that BAPTA attenuates EPSCs to a similar extent throughout the developmental period (Fedchyshyn & Wang, 2005). As the Ca^{2+}-binding rate of EGTA is two orders of magnitude slower than that of BAPTA (Smith *et al.* 1984), it has been proposed that the number of VGCCs comprising the Ca^{2+} domain may decrease during development (Fedchyshyn & Wang, 2005). The intraterminal Ca^{2+} dynamics may also change as a result of developmental increase in endogenous Ca^{2+} buffers (Lohmann & Friauf, 1996; Felmy & Schneggenburger,

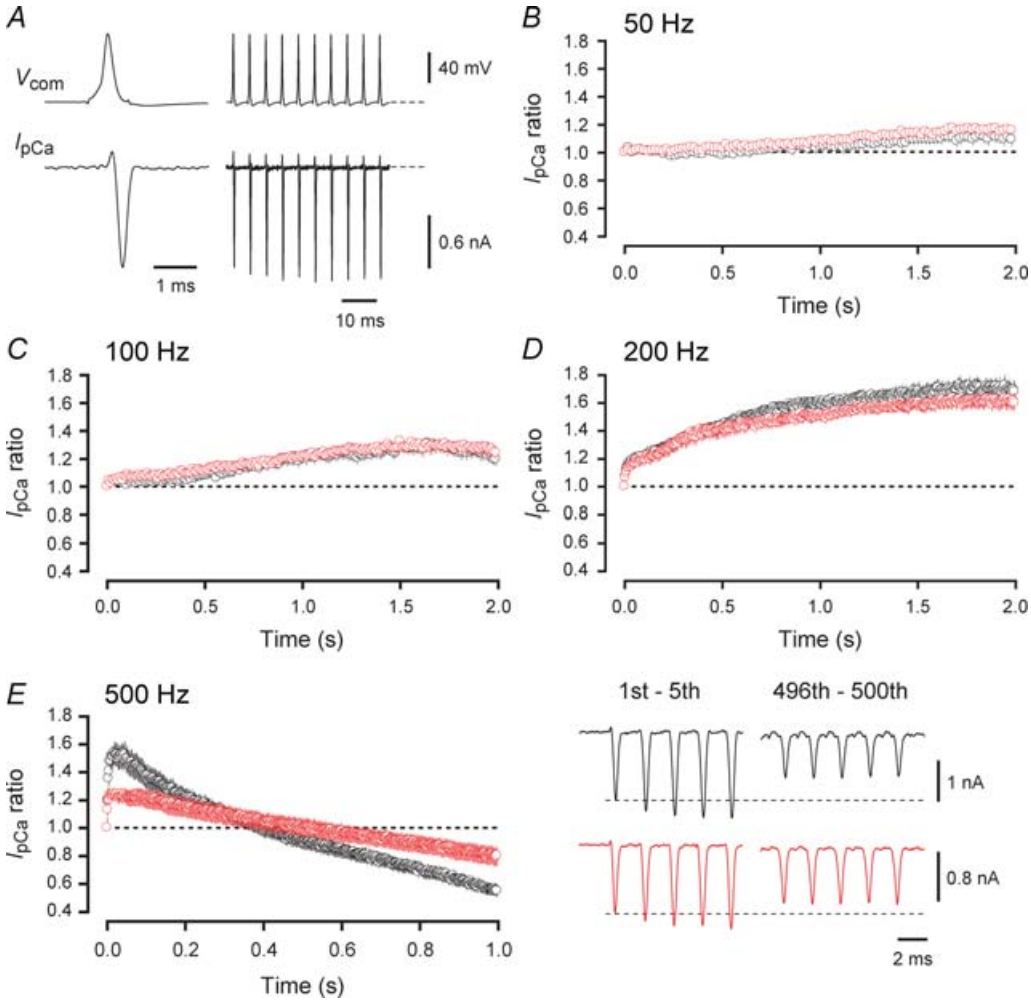

Figure 6. Involvement of CaM in activity-dependent inactivation and facilitation of I_{pCa} at P13–15 calyces
A, sample records of I_{pCa} evoked by 200 Hz trains of AP-waveform command pulses (V_{com}). The AP-waveforms were obtained from another calyceal terminal at the resting potential of −71 mV. The initial AP (shown on a fast time scale) had an overshoot of 22 mV. *B–E*, the I_{pCa} amplitude, normalized to the first one, during 50 Hz (*B*), 100 Hz (*C*), 200 Hz (*D*) and 500 Hz (*E*) trains, in the presence (red) and absence (black) of MLCK peptide (30 μM) in the calyceal terminal. Averaged data are from 4 to 5 calyceal terminals. Sample records in *E* show the 1st–5th and 496th–500th I_{pCa} during 500 Hz trains, in the absence (black traces) and presence (red traces) of MLCK peptide. The maximal I_{pCa} facilitation and inactivation was 55.2 ± 5.3% and 45.9 ± 4.9%, respectively, in control ($n = 5$), and 27 ± 4.2% ($P < 0.03$) and 21.3 ± 6.2% ($P < 0.02$), respectively, in the presence of MLCK peptide ($n = 4$).

2004), or more restricted Ca^{2+} diffusion owing to the developmental restructuring of calyces (Kandler & Friauf, 1993; Taschenberger *et al.* 2002).

Ca^{2+}-dependent Ca^{2+} current facilitation

At P13–15 calyces, during repetitive stimulation (50–500 Hz), I_{pCa} showed facilitation as reported previously (Cuttle *et al.* 1998; Forsythe *et al.* 1998; Taschenberger *et al.* 2002; Tsujimoto *et al.* 2002). This facilitation could be attenuated by 10 mM EGTA (Fig. 5*B*), but the CaM inhibitor MLCK peptide had no effect on the facilitation evoked by AP-waveform command pulses at 50–200 Hz. Given that neuronal calcium sensor 1 (NCS-1) mimics and partially occludes I_{pCa} facilitation produced by a pair of depolarizing pulses at 5–20 ms intervals (Tsujimoto *et al.* 2002), Ca^{2+}-dependent I_{pCa} facilitations observed at 50–200 Hz is likely to be mediated by NCS-1. During 500 Hz stimulation, however, MLCK peptide attenuated I_{pCa} facilitation, suggesting an additional involvement of CaM at this maximal frequency. These observations are in agreement with the fact that NCS-1 has more than 10 times higher Ca^{2+}-binding affinity than CaM (Burgoyne, 2007). Among EF-hand splice variants of VGCC α_{1A} subunit, EF_a channels are sensitive to global changes in intracellular Ca^{2+} concentration, whereas EF_b channels are insensitive, being spared even in the presence of 10 mM BAPTA (Chaudhuri *et al.* 2004). Thus, EF_a channels are more likely to be involved in the facilitation of I_{pCa} at the calyx of Held.

Physiological roles of CaM-dependent I_{pCa} modulations

At calyceal synapses in the prehearing period, with non-dialysed presynaptic terminals, synaptic depression induced by repetitive stimulation of afferent fibres was attenuated by calmidazolium. Ca^{2+}/CaM is thought to accelerate vesicle replenishment at calyceal synapses (Sakaba & Neher, 2001). If this mechanism predominates, the CaM blocker should have increased the magnitude of depression. Thus, Ca^{2+}/CaM-dependent I_{pCa} inactivation seems to be a more important mechanism underlying synaptic depression during low frequency stimulation (< 30 Hz) at the immature calyx of Held, as postulated by Xu & Wu (2005). However, at posthearing calyces Ca^{2+}/CaM-dependent I_{pCa} inactivation became evident only after prolonged high frequency stimulation. At calyceal synapses of P15 mice, at room temperature, transmission starts to fail at 20 Hz and failures become prominent at 50 Hz, unless NMDA receptors are pharmacologically blocked (Futai *et al.* 2001). In this respect, Ca^{2+}/CaM-dependent I_{pCa} inactivation during prolonged transmission at 500 Hz is unlikely to play a physiological role. It remains to be seen, however, whether this mechanism operates for synaptic depression in physiological conditions. At physiological temperature, calyceal synapses can follow short trains of afferent fibre stimulations at 600–800 Hz (Taschenberger & von Gersdorff, 2000), but the build-up of intraterminal Ca^{2+} may be reduced by faster activation/inactivation kinetics of I_{pCa} (Kushmerick *et al.* 2006).

Short-term synaptic depression at immature calyces, before hearing onset, involves multiple mechanisms, in addition to classically documented depletion of releasable synaptic vesicles (Betz, 1970). These mechanisms include desensitization of postsynaptic AMPA receptors (Taschenberger *et al.* 2002, 2005), autoreceptor inhibition via G protein-coupled receptors (Iwasaki & Takahashi, 2001; Kimura *et al.* 2003) and Ca^{2+}/CaM-dependent I_{pCa} inactivation (Xu & Wu, 2005; present study). As animals mature, most of these mechanisms become less significant, with vesicle depletion remaining as the most important mechanism underlying short-term depression at the calyx of Held.

References

Betz WJ (1970). Depression of transmitter release at the neuromuscular junction of the frog. *J Physiol* **206**, 629–644.

Borst JGG & Sakmann B (1996). Calcium influx and transmitter release in a fast CNS synapse. *Nature* **383**, 431–434.

Borst JGG & Sakmann B (1998). Facilitation of presynaptic calcium currents in the rat brainstem. *J Physiol* **513**, 149–155.

Burgoyne RD (2007). Neuronal calcium sensor proteins: generating diversity in neuronal Ca^{2+} signalling. *Nat Rev Neurosci* **8**, 182–193.

Chaudhuri D, Chang S-Y, DeMaria CD, Alvania RS, Soong TW & Yue DT (2004). Alternative splicing as a molecular switch for Ca^{2+}/calmodulin-dependent facilitation of P/Q-type Ca^{2+} channels. *J Neurosci* **24**, 6334–6342.

Cuttle MF, Tsujimoto T, Forsythe ID & Takahashi T (1998). Facilitation of the presynaptic calcium current at an auditory synapse in rat brainstem. *J Physiol* **512**, 723–729.

DeMaria CD, Soong TW, Alseikhan BA, Alvania RS & Yue DT (2001). Calmodulin bifurcates the local Ca^{2+} signal that modulates P/Q-type Ca^{2+} channels. *Nature* **411**, 484–489.

Fedchyshyn MJ & Wang LY (2005). Developmental transformation of the release modality at the calyx of Held synapse. *J Neurosci* **25**, 4131–4140.

Felmy F & Schneggenburger R (2004). Developmental expression of the Ca^{2+}-binding proteins calretinin and parvalbumin at the calyx of Held of rats and mice. *Eur J Neurosci* **20**, 1473–1482.

Forsythe ID, Tsujimoto T, Barnes-Davies M, Cuttle MF & Takahashi T (1998). Inactivation of presynaptic calcium current contributes to synaptic depression at a fast central synapse. *Neuron* **20**, 797–807.

Futai K, Okada M, Matsuyama K & Takahashi T (2001). High-fidelity transmission acquired via a developmental decrease in NMDA receptor expression at an auditory synapse. *J Neurosci* **21**, 3342–3349.

Helmchen F, Borst JGG & Sakmann B (1997). Calcium dynamics associated with a single action potential in a CNS presynaptic terminal. *Biophys J* **72**, 1458–1471.

Inchauspe CG, Martini FJ, Forsythe ID & Uchitel OD (2004). Functional compensation of P/Q by N-type channels blocks short-term plasticity at the calyx of Held presynaptic terminal. *J Neurosci* **24**, 10379–10383.

Ishikawa T, Kaneko M, Shin H-S & Takahashi T (2005). Presynaptic N-type and P/Q-type Ca^{2+} channels mediating synaptic transmission at the calyx of Held of mice. *J Physiol* **568**, 199–209.

Ishikawa T, Nakamura Y, Saitoh N, Li W-B, Iwasaki S & Takahashi T (2003). Distinct roles of Kv1 and Kv3 potassium channels at the calyx of Held presynaptic terminal. *J Neurosci* **23**, 10445–10453.

Iwasaki S, Momiyama A, Uchitel OD & Takahashi T (2000). Developmental changes in calcium channel types mediating central synaptic transmission. *J Neurosci* **20**, 59–65.

Iwasaki S & Takahashi T (1998). Developmental changes in calcium channel types mediating synaptic transmission in rat auditory brainstem. *J Physiol* **509**, 419–423.

Iwasaki S & Takahashi T (2001). Developmental regulation of transmitter release at the calyx of Held in rat auditory brainstem. *J Physiol* **534**, 861–871.

Jewett DL & Romano MN (1972). Neonatal development of auditory system potentials averaged from the scalp of rat and cat. *Brain Res* **36**, 101–115.

Kandler K & Friauf E (1993). Pre- and postnatal development of efferent connections of the cochlear nucleus in the rat. *J Comp Neurol* **328**, 161–184.

Kimura M, Saitoh N & Takahashi T (2003). Adenosine A_1 receptor-mediated presynaptic inhibition at the calyx of Held of immature rats. *J Physiol* **553**, 415–426.

Kushmerick C, Renden R & von Gersdorff H (2006). Physiological temperatures reduce the rate of vesicle pool depletion and short-term depression via an acceleration of vesicle recruitment. *J Neurosci* **26**, 1366–1377.

Lee A, Scheuer T & Catterall WA (2000). Ca^{2+}/calmodulin-dependent facilitation and inactivation of P/Q-type Ca^{2+} channels. *J Neurosci* **20**, 6830–6838.

Liang H, DeMaria CD, Erickson MG, Mori MX, Alseikhan BA & Yue DT (2003). Unified mechanisms of Ca^{2+} regulation across the Ca^{2+} channel family. *Neuron* **39**, 951–960.

Lohmann C & Friauf E (1996). Distribution of the calcium-binding proteins parvalbumin and calretinin in the auditory brainstem of adult and developing rats. *J Comp Neurol* **367**, 90–109.

Nakamura Y, DiGregorio D & Takahashi T (2007). Single action potential-evoked Ca^{2+} transients at the calyx of Held presynaptic terminal. *Neurosci Res* **58S**, S71.

Sakaba T & Neher E (2001). Calmodulin mediates rapid recruitment of fast-releasing synaptic vesicles at a calyx-type synapse. *Neuron* **32**, 1119–1131.

Shifman JM, Choi MH, Mihalas S, Mayo SL & Kennedy MB (2006). Ca^{2+}/calmodulin-dependent protein kinase II (CaMKII) is activated by calmodulin with two bound calciums. *Proc Natl Acad Sci U S A* **103**, 13968–13973.

Smith PD, Liesegang GW, Berger RL, Czerlinski G & Podolsky RJ (1984). A stopped-flow investigation of calcium ion binding by ethylene glycol bis (b-aminoethyl ether)-N,N-tetraacetic acid. *Anal Biochem* **143**, 188–195.

Takahashi T (2005). Dynamic aspects of presynaptic calcium currents mediating synaptic transmission. *Cell Calcium* **37**, 507–511.

Takahashi T, Hori T, Kajikawa Y & Tsujimoto T (2000). The role of GTP-binding protein activity in fast central synaptic transmission. *Science* **289**, 460–463.

Taschenberger H, Leão RM, Rowland KC, Spirou GA & von Gersdorff H (2002). Optimizing synaptic architecture and efficiency for high-frequency transmission. *Neuron* **36**, 1127–1143.

Taschenberger H, Scheuss V & Neher E (2005). Release kinetics, quantal parameters and their modulation during short-term depression at a developing synapse in the rat CNS. *J Physiol* **568**, 513–537.

Taschenberger H & von Gersdorff H (2000). Fine-tuning an auditory synapse for speed and fidelity: developmental changes in presynaptic waveform, EPSC kinetics, and synaptic plasticity. *J Neurosci* **20**, 9162–9173.

Török K & Trentham DR (1994). Mechanism of 2-chloro-(ε-amino-Lys75)-[6-[4-(N,N-diethylamino)phenyl]-1,3,5-triazin-4-yl]calmodulin interactions with smooth muscle myosin light chain kinase and derived peptides. *Biochemistry* **33**, 12807–12820.

Tsujimoto T, Jeromin A, Saitoh N, Roder JC & Takahashi T (2002). Neuronal calcium sensor 1 and activity-dependent facilitation of P/Q-type calcium currents at presynaptic nerve terminals. *Science* **295**, 2276–2279.

Xu J & Wu L-G (2005). The decrease in the presynaptic calcium current is a major cause of short-term depression at a calyx-type synapse. *Neuron* **46**, 633–645.

Yamashita T, Ishikawa T & Takahashi T (2003). Developmental increase in vesicular glutamate content does not cause saturation of AMPA receptors at the calyx of Held synapse. *J Neurosci* **23**, 3633–3638.

Acknowledgements

This study was supported by a Grant-in-Aid for Specially Promoted Research from the Ministry of Education, Culture, Sports, Science and Technology to T.T. and Research Fellowship from the Japanese Society for the Promotion of Science to T.Y. We thank Mark Farrant for helpful comments and Masahiro Kaneko for providing action-potential waveform command templates.